SYNTHESIS OF TiO_2-M (Cd, Co, Mn) AS A PHOTOCATALYST DEGRADATION OF METHYLENE BLUE DYE

Candra Purnawan, Sayekti Wahyuningsih, Dwita Nur Aisyah
Sebelas Maret University (Indonesia)

Abstract. TiO_2-M (M = Cd, Co, Mn) were synthesized by sol-gel method using titanium(IV) isopropoxide (TTIP) and cadmium sulfate octahydrate ($CdSO_4.8H_2O$), manganese(II) sulfate monohydrate ($MnSO_4.H_2O$), cobalt(II) sulfate heptahydrate ($CoSO_4.7H_2O$) as precursors. M-doped TiO_2 was performed with molar ratio 1:3; 1:2; 1:1; 2:1; 3:1 (mol Ti / mol M) and photocatalytic processes using visible light with irradiation time for 5, 10, 15, 20, 25 and 30 minutes. This study was carried out to determine the effect of different metal ions, the composition of Ti:M and the exposure time on the photocatalytic degradation of methylene blue dye. The results showed that different metal ions influenced crystal size and affected electronic properties (band gap). Crystal size of TiO_2 > TiO_2-Mn > TiO_2-Co > TiO_2-Cd and band gap of TiO_2 > TiO_2-Cd > TiO_2-Co > TiO_2-Mn. In addition, differences of Ti:M composition also influenced the photocatalytic activity. The longer of applied time exposure, the higher photocatalytic degradation of methylene blue was achieved. The optimum composition of Ti:M was obtained at Ti:M ratio by 3:1 with degradation values by 92.56% (TiO_2-Cd), 90.44% (TiO_2-Co), and 89.42% (TiO_2-Mn).

Keywords: methylene blue; metal doping; photocatalytic degradation; TiO_2-M; visible light

Introduction

Indonesia is one of textile industrial based country producing wastewater. Most of wastewater generated from textile industry contain dyes which difficult to eliminate and to degrade. One of dyes often used in textile industry is methylene blue. Methylene blue, one of cationic dyes with chemical formula $C_{16}H_{18}ClN_3S$, is frequently employed in cotton, paper and hair dying process (Alzaydien, 2009). This aromatic hydrocarbon compound has strong adsorption and it was categorized as thiazine dyes. It also has toxic properties causing some effects in health, including skin irritation, cyanosis, and gastrointestinal track irritation (Hamdaoui & Chiha, 2007).

Nowadays, the researchers utilized TiO_2 semiconductor to degrade the dyes through photocatalytic, electrocatalyst, and photoelectrocatalyst degradation meth-

ods (Hamadanian et al., 2010; Purnawan et al., 2016; Wahyuningsih et al., 2013). The use of photocatalyst material, however, is limited since it only absorbs 5% ultraviolet light from sun with broad band gap: 3.0 – 3.2 eV (Ni et al., 2007). Thus, modification is required to improve optical property in visible light range.

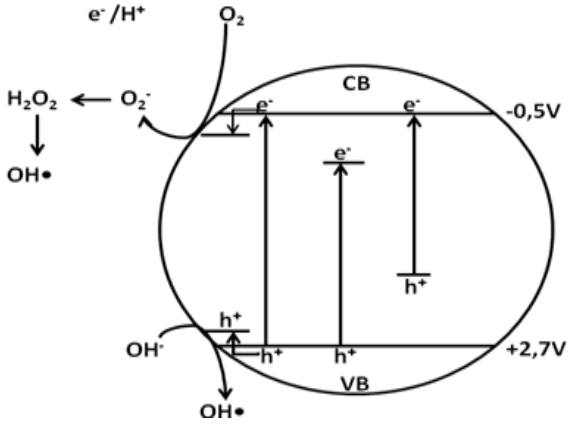

Figure 1. Photocatalytic mechanism of TiO_2 (hv_1 = origin TiO_2, hv_2 = metals ion doped TiO_2, hv_3 = non-metal doped TiO_2) (Zaleska, 2008)

Modification of TiO_2 can be performed by adding metals or doping metals like transition metals (Binas et al., 2012; Chen et al., 2005; Deng et al., 2011; Purnawan et al., 2016). The addition of metals into TiO_2 semiconductor with increasing concentration caused lowering band gap energy up to visible light absorption area (Ganesh et al., 2012; Tian et al., 2012).

Dopant ion formed electron trapping which it minimizes recombination process between electron and hole. Not only it resulted new band gap, metal doping also accelerated photocatalytic activities (El-Bahy et al., 2009; Zaleska, 2008). Fig. 1 illustrated the effect of metals doping on electron excitation of TiO_2 photocatalyst.

The addition of metals into TiO_2 semiconductor will decrease the particle size of doped semiconductor compared to the origin one. Introducing Cd metal into TiO_2 affected in lowering band gap of TiO_2/CdS (Li et al., 2014) and enhanced its photocatalytic activities in visible light (Shi et al., 2012). The decreasing of TiO_2 band gab and enhancing of its photocatalytic activities in visible light was also reported by adding Co (Miao et al., 2014; Yang et al., 2007) and Mn metals (Binas et al., 2012; Deng et al., 2011; Papadimitriou et al., 2011; Wang et al., 2015). The dopant Mn decreased the band gap thus it can be adsorbed the visible light. However, it could defect the TiO_2 crystal and reduce the photocatalytic activities when Mn metal was added in high concentration (Deng et al., 2011).

The TiO_2 doped with Mn (0.1%, 1% and 5%) degraded the methylene blue up to 70% by irradiating in visible light for 30 minutes (Binas et al., 2012; Papadimitriou et al., 2011). Another researcher, Wang et al. (2015), obtained optimum result by doping 6% Mn to TiO_2. They also found that by increasing Mn concentration increased the rutile phase which reduce the TiO_2 photocatalytic sensitivity. However, the comparative study of three kind of metals, Co, Cd and Mn, doping TiO_2 is not yet studied. Thus, in this research successfully prepared the TiO_2 doped metals (Co, Cd and Mn) and evaluated their photocatalytic performance on methylene blue degradation.

Experimental

Materials and instrument

All reagents employed in this research were commercially available from E-Merck except mentioned. They were titanium(IV) isopropoxide (TTIP), $CdSO_4.8H_2O$, $MnSO_4.1H_2O$, $CoSO_4.7H_2O$, acetic acid glacial, and ethanol. The methylene blue dye was commercially available from Surakarta, Indonesia. Aquades was purchased from Chemistry Laboratory of Universitas Sebelas Maret. The Instruments used in this study were XRD (*X-Ray Diffraction*, Bruker), SEM-EDX (*Scanning Electron Microscopy – Energy Dispersive X-ray*), FTIR (*Spektrofotometer Fourier Transform Infrared*, Shimadzu 6000) and *visible* lamp osram ultra vitalux (300W 230V AC).

Synthesis of TiO_2-M (Cd, Mn, Co)

Titanium (IV) isopropoxide solution was hydrolyzed in acetic acid glacial solution at 14 ºC with solution ration 1:10 v/v. The mixture was stirred continuously until the white and viscous solution achieved. Then, it was heated at 90 ºC to obtain white gel form. Afterward, each $CdSO_4$, $MnSO_4$ or $CoSO_4$ solutions was added drop wise into TiO_2 gel. The ratio of each metal sulfate toward TiO_2 gel was 1:3, 1:2, 1:1, 2:1 and 3:1 mol/mol. After it was cooled at room temperature, the gel was dried at 150 ºC for 24 h, then calcined at 400 ºC at 2 h.

Photocatalytic degradation of methylene blue

Photodegradation of methylene blue was conducted by adding 0.3 g TiO_2-M powder into 30 mL of 5 $mg.L^{-1}$ methylene blue solution. Under stirring condition, the mixture was irradiated with visible light in Black Box reactor. The visible light irradiation was carried out at 5, 10, 15, 20, 25 and 30 minutes. Afterward, the solution was separated using centrifugation at 6000 rpm for around 3 minutes. The solution absorbance was then analyzed using UV-Vis spectrophotometer.

Results and discussion

Characterization of crystal structure and size by XRD

The XRD characterization of TiO_2-M was conducted to evaluate crystallinity of TiO_2-M powder by comparing the samples diffractogram with JCPDS standard. It

was carried out on the 3:1 (TiO_2:M) ratio of synthesized TiO_2-M at 2thetha 15–85°. Based on the XRD spectra of TiO_2-M (3:1) showed in Fig. 2 can be seen the primary characteristic peak of TiO_2 at 2θ 25.490°, 37.792° and 48.043°. This peak was confirmed as anatase phase corresponding to JCPDS number 78-2486. This anatase peak was also observed in TiO_2-Cd, TiO_2-Co and TiO_2-Mn diffractograms.

Table 1. The crystal size of TiO_2 and TiO_2-M

Material	Crystal size (nm)
TiO_2-Cd	6,907
TiO_2-Co	7,223
TiO_2-Mn	7,404
TiO_2	15,622

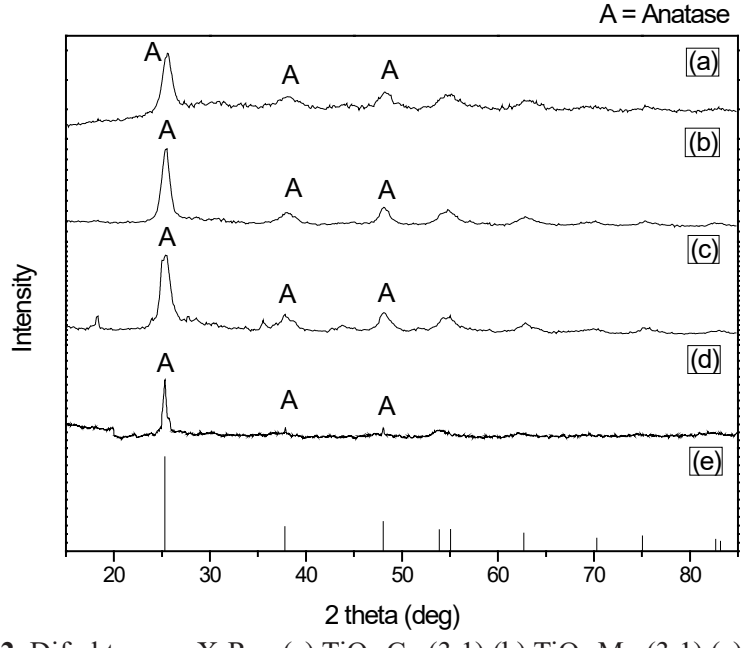

Figure 2. Difraktogram X-Ray (a) TiO_2-Co (3:1) (b) TiO_2-Mn (3:1) (c) TiO_2-Cd (3:1) (d) TiO_2 (e) JCPDS TiO_2 No 78-2486

The addition of metals into TiO_2 influenced the product crystal size. All of the TiO_2-M crystal size was lower than TiO_2. Comparing to another TiO_2-M, the TiO_2-Cd was the synthesized product having lowest crystal size, as shown in Table 1. This phenomena was also discovered by Deng et al. (2011), where after Mn metals was doped into TiO_2, it resulted 7 nm of TiO_2-Mn crystal size.

Morphological study of TiO$_2$-M

Morphological study of TiO$_2$-Cd, TiO$_2$-Mn and TiO$_2$-Co was conducted at each TiO$_2$:M ratio by 3:1. All of the TiO$_2$-M surface morphology was offered in Fig. 3. All of the measurement were captured at magnificent 5000x. The morphology of TiO$_2$-M was not significantly different observed in this research. This indicated that the addition of metals was not change the morphology of TiO$_2$-M. From the SEM image was calculated the particle size distribution using JImage application. The calculation result gave same values, where the particle size of TiO$_2$-M was distributed in range of 100-200 nm. Fig. 4 revealed the particle size distribution of each TiO$_2$-M.

The SEM-EDAX result showed that the doped metal concentration contained in TiO$_2$-M as presented in Table 2 were 8.62, 3.26 and 7.21% for Cd, Co and Mn, respectively. It was mean that the Cd was easily doped into TiO$_2$ than Co or even Mn. This was caused by the ionic radius of Cd was higher than Co and Mn, however its covalent radius of ionic hydrant was smaller than others, i.e. Cd (144±9 pm) < Co (150±7 pm) < Mn (161±8 pm). Due to it has small covalent radius of ionic hydrant, the Cd ion was readily to bind and to attach into TiO$_2$ semiconductor.

Table 2. Elemental analysis of TiO$_2$-M generated from SEM-EDAX

Elements	Composition (%)		
	TiO$_2$-Cd	TiO$_2$-Mn	TiO$_2$-Co
C	5,76	4,59	6,13
O	29,50	38,14	33,53
M (Cd, Mn or Co)	8,62	3,26	7,21
Ti	53,54	51,85	51,83

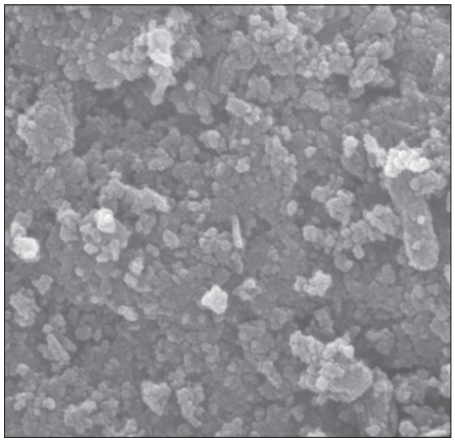

(a)

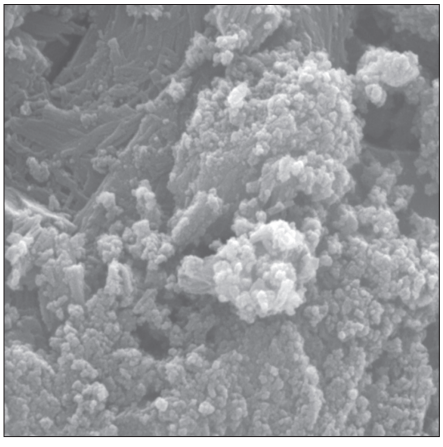

(b)

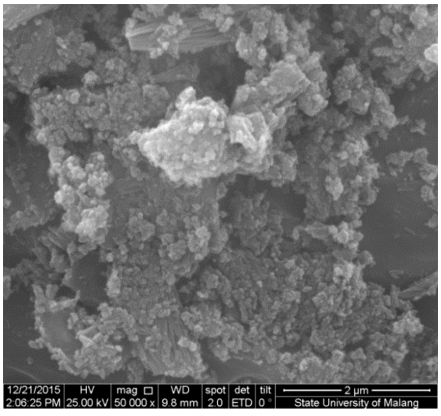

(c)

Figure 3. Morphology of (a) TiO_2-Cd, (b) TiO_2-Mn and (c) TiO_2-Co

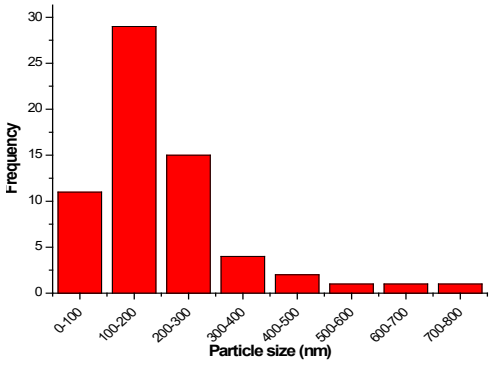

(a)

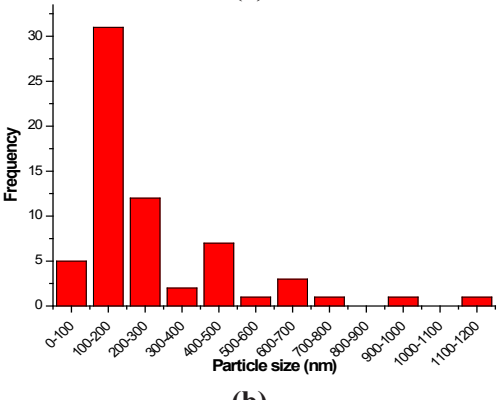

(b)

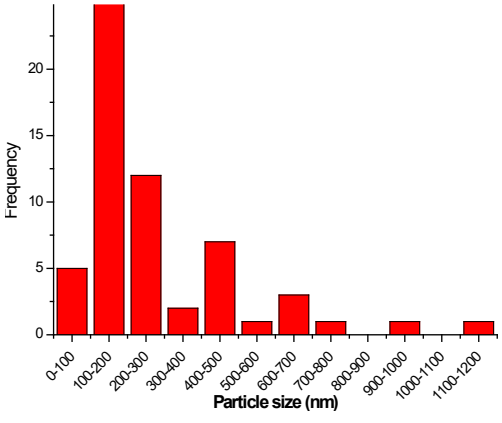

(c)

Figure 4. Particle size distribution of (a) TiO_2-Cd, (b) TiO_2-Mn and (c) TiO_2-Co

Band gap energy

The band gap energy was conducted via thin layer method. The TiO_2 and TiO_2-M samples was transformed to the transparency film at glass substrate then their absorbance were recorded using UV-Vis spectrophotometer. The band gap was calculated using Touc Plot method, a method to determine band gap using extrapolate from E (eV) versus $(Ahv)^2$ as shown in Fig. 5. Based on the Touch Plot graph can be evaluated band gap energy of each samples presented in Table 3.

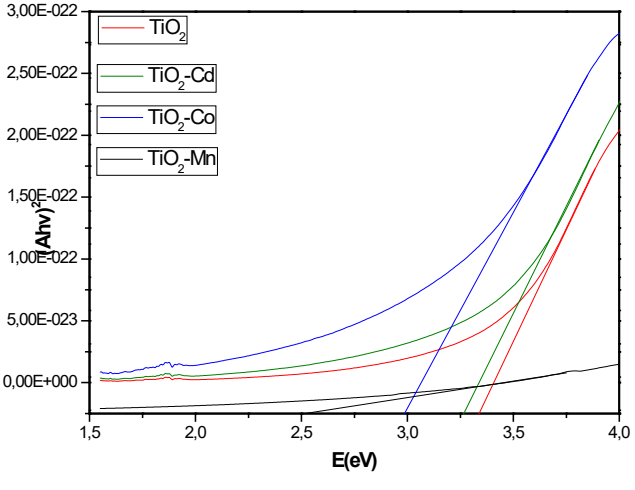

Figure 5. *Touc plot* graph of TiO_2 and TiO_2-M (3:1)

Table 3. The *band gap* and wave length values of TiO_2-M (3:1)

Sampel	Band gap (eV)	λ (nm)
TiO_2	3,35	370,15
TiO_2-Cd	3,15	393,65
TiO_2-Co	3,00	413,33
TiO_2-Mn	2,5	496,00

The addition of metals into TiO_2 triggered the lowering band gap energy as presented in Table 3, the Eg of TiO_2> TiO_2-Cd > TiO_2-Co > TiO_2-Mn. The band gap energy of TiO_2-Mn was lowest to others TiO_2-M. This initiated a fast recombination of electron-hole which will inhibit oxidation reaction of methylene blue dye.

FTIR analysis of TiO_2M

Analysis of TiO_2-Cd using FTIR was performed to identify a bonding between Ti-O and Cd as result of Cd addition to TiO_2. In Fig. 6, the synthesized TiO_2 spectra has absorbance bands around 3405.47 cm^{-1}, 1627.99 cm^{-1} as well as strong and broad band at 576.74 – 421.46 cm^{-1} which they are characteristic band of TiO_2. The wave number at 3405.47 cm^{-1} indicated the O-H stretching vibration of water entrapping in TiO_2 structure (Kuvarega et al., 2011). Another characteristic peak of water was also observed around 1625 – 1650 cm^{-1} corresponding to the O-H bending vibration. The vibration of O-Ti-O was also discovered in the IR spectra at around 609.5 – 420.5 cm^{-1} (Wahyuningsih et al., 2013).

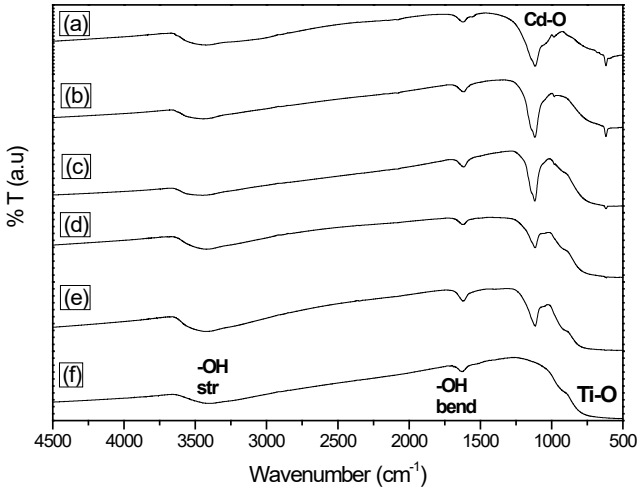

Figure 6. IR spectra of TiO_2-Cd, with ratio (a) 1:3 (b) 1:2 (c) 1:1 (d) 2:1 (e) 3:1, dan (f) TiO_2

The IR spectrum of TiO_2-Cd showed the broad absorbance band at around 3400 cm^{-1} indicating the O-H stretching vibration (Kuvarega et al., 2011). The water characteristic band was also observed in TiO_2-Cd IR spectra appearing at 1600 cm^{-1} (Li et al., 2011; Wu & Chen, 2004). A new absorbance band also appeared around 1115 – 1057 cm^{-1} indicated the Ti-O-Cd stretching vibration. In addition, the absorbance band around 540 – 425 cm^{-1} corresponding to Ti-O-Cd bending vibration. Both of this peaks were sharpen by decreasing of TiO_2: Cd ratio. This peaks related to the Ti-O-Cd bonding formation as result of Cd insertion in TiO_2.

The two peaks around 1100 cm^{-1} and 980 cm^{-1} were characteristic peak of Ti-O-Cd stretching vibration in accordance with what has been done by Ge (2012). Both of that peaks showed different intensity on each TiO_2: Cd composition ratio, the more concentration of Cd was added then the peak became sharpen. This also occurred at peak around 619.18 – 618.21 cm^{-1} which corresponding to Cd stretching vibration.

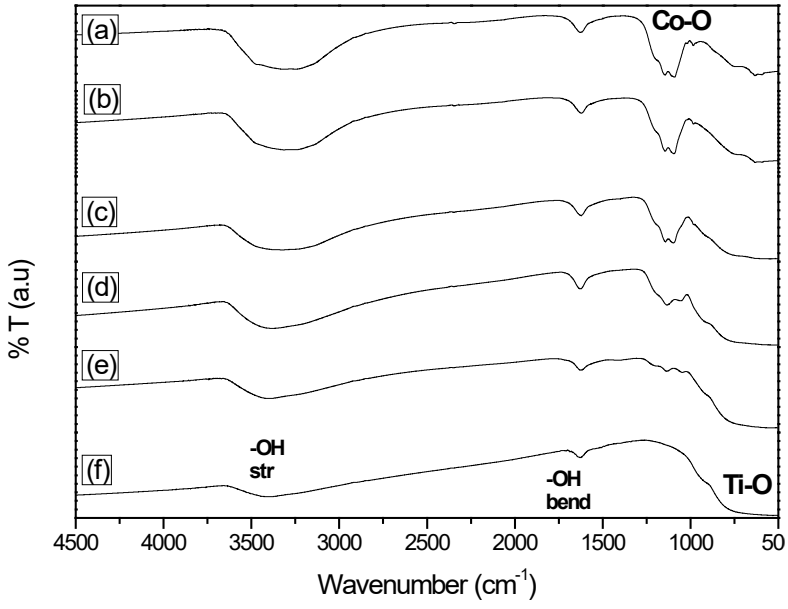

Figure 7. The TiO_2-Co IR spectrum at TiO_2 : Co ratio (a) 1:3 (b) 1:2 (c) 1:1 (d) 2:1 (e) 3:1, and (f) TiO_2

In TiO_2-Co IR spectra offered in Fig. 7 revealed a peak at 1627 cm^{-1} corresponding to a bending vibration of H-O-H bonding. Peaks around 600 – 400 cm^{-1} was an absorbance band of Ti-O-Ti. It was also exposed a weak and broad band around 2840 cm^{-1} becoming strong peak by adding more Co, indicate the OH absorbance band of H_2O bonded to Co-O. Absorbance band around 1000 – 1250 cm^{-1} was a

characteristic peak of Co evidenced by increasing of its intensity with addition more concentration of Co while weaken by decreasing of Co composition (Ganesh et al., 2012).

A new absorbance band at 660 cm^{-1} was found in TiO_2-Mn spectra presented in Fig. 8 indicating the β-MnO_2 vibration. Moreover, peaks at 620 cm^{-1} and 530 cm^{-1} was a characteristic vibration of O-Ti-O and Mn-O-Ti, respectively. Identification of MnO_x was difficult to evaluate due to this peak over lapped with other peaks. This was also observed by other researchers (Kernazhitsky et al., 2010; Othman et al., 2007; Šurca et al, 2006). However, a peak around 1140–997 cm^{-1} was predicted as Mn-O characteristic absorbance band since its intensity became sharpen at high ratio of Cd.

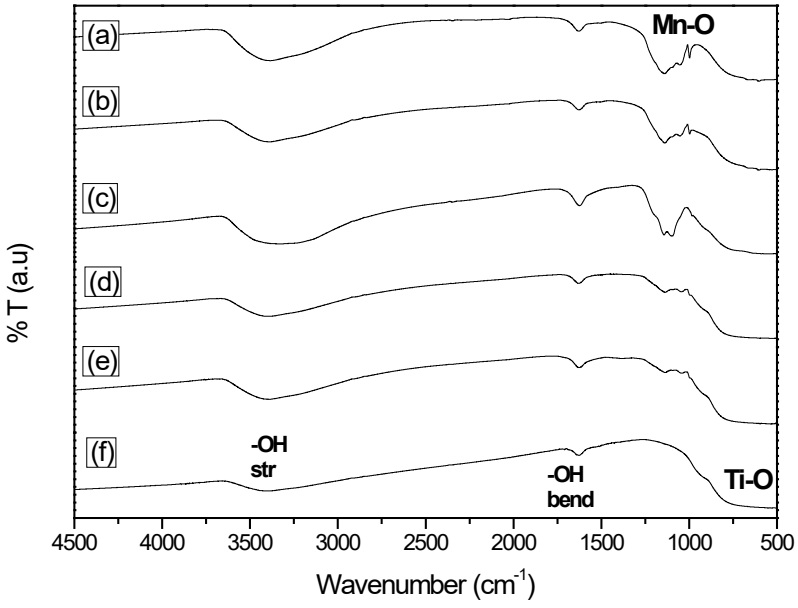

Figure 8. TiO_2-Mn IR spectrum with TiO_2 : Mn ratio (a) 1:3 (b) 1:2 (c) 1:1 (d) 2:1 (e) 3:1, and (f) TiO_2

Photocatalytic degradation of methylene blue

Qualitative analysis of methylene blue using UV-Vis spectrophotometer was conducted to determine its maximum wavelength (λ_{maks}). It was scanned in range of 800 nm – 350 nm with methylene blue concentration by 5 $mg.L^{-1}$. It was resulted that the maximum wavelength was obtained at 664 nm. This maximum wavelength was then used to identify the decreasing of methylene blue concentration in aqueous solution after photocatalytic degradation carried out.

This research focused to compare the photocatalytic activity of each TiO_2-M using visible light at same time and amount. After photocatalytic degradation, it was observed that the absorbance of methylene blue decreased. Photocatalytic degradation is a reaction process involved catalyst assisted with a photon. Fig. 9 showed the degradation result of each TiO_2-Cd composition. All of composition revealed that the longer of contact time, the degradation percentages enhanced. They resulted a degradation closing to 90% at 30 minutes. The role on photocatalytic degradation was obtained as follow TiO_2-Cd (3:1) > (2:1) > (1:3) > (1:2) > (1:1). The same pattern was also discovered for TiO_2-Co and TiO_2-Mn where the highest degradation percentages was achieved at TiO_2:M ratio 3:1 while the lowest was at 1:1. The percentage degradation data of TiO_2-Co and TiO_2-Mn were presented in Fig. 10 and Fig. 11, respectively.

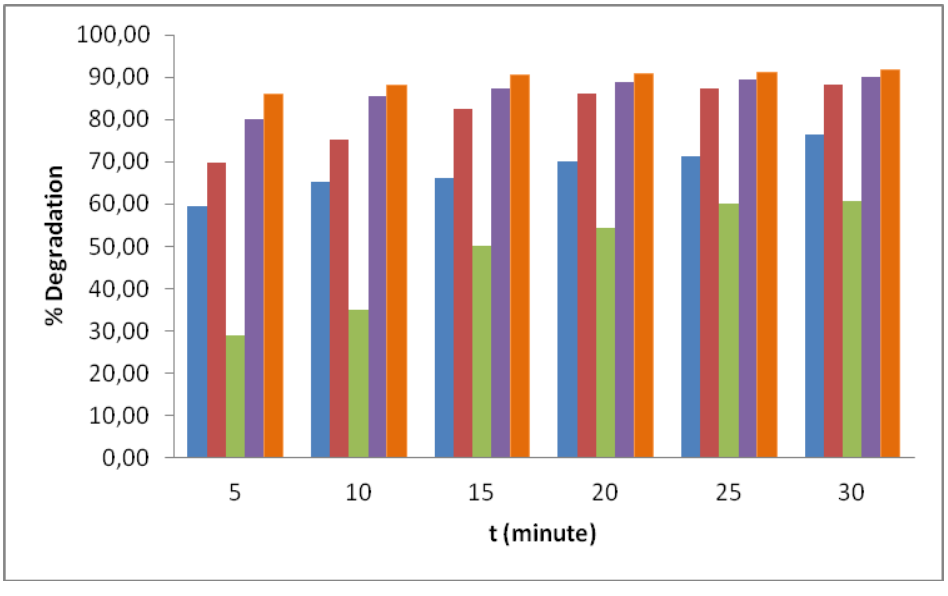

Figure 9. Methylene blue degradation percentages using TiO_2-Co at ratio TiO_2:Co = 1:3 (blue); 1:2 (red); 1:1 (green); 2:1 (violet) and 3:1 (orange)

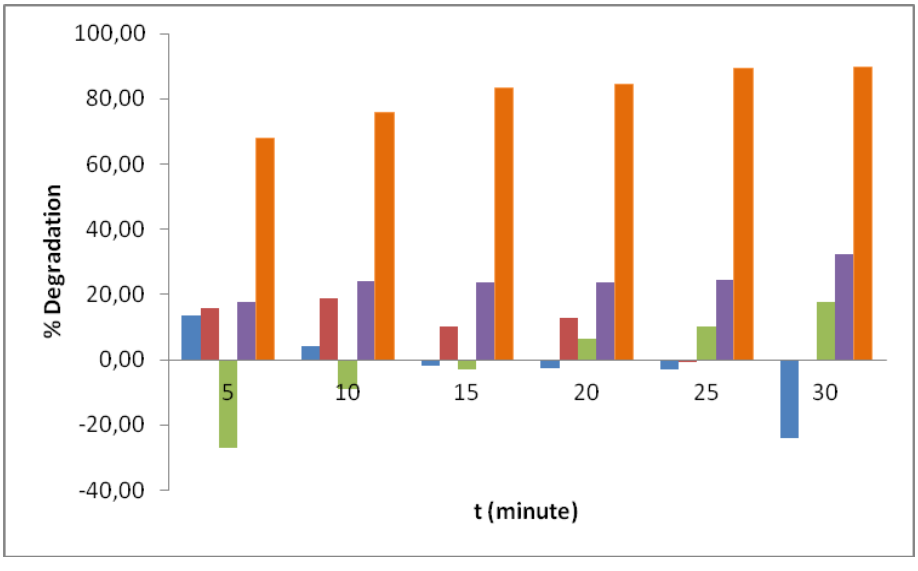

Figure 10. Methylene blue degradation percentages using TiO_2-Mn at ratio TiO_2:Mn = 1:3 (blue); 1:2 (red); 1:1 (green); 2:1 (violet) and 3:1 (orange)

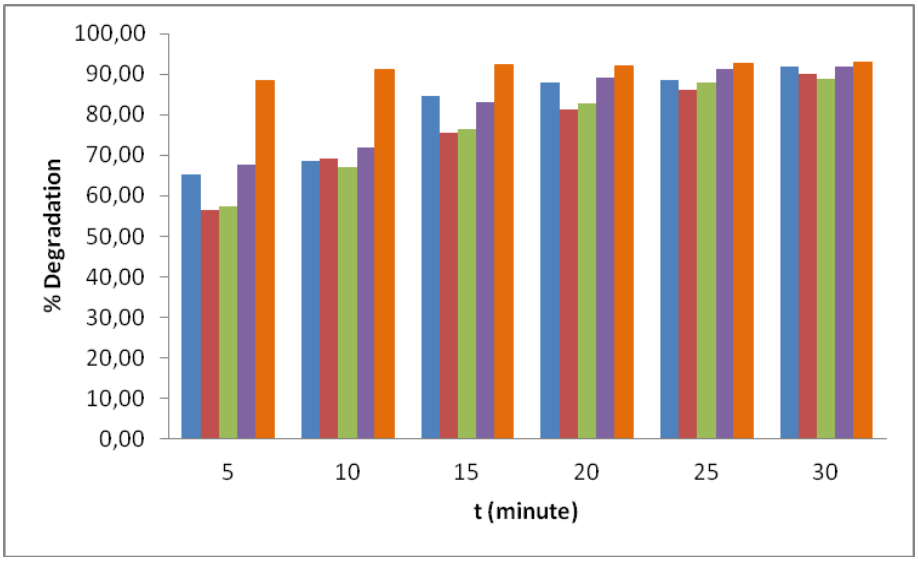

Figure 11. Methylene blue degradation percentages using TiO_2-Cd at ratio TiO_2:Cd = 1:3 (blue); 1:2 (red); 1:1 (green); 2:1 (violet) and 3:1 (orange)

The addition of high concentration of metals caused on decreasing of photocatalytic activity. High metal concentration has high number of defect structure and created more trapper. It triggered a charge carrier generated from energy induction result on TiO_2 photocatalyst can stuck more than one time thus it slow down the mobility and it could undergo a recombination before reaching photocatalyst surfaces. This phenomena initiating at high composition of dopant resulted low degradation percentage compared to a sample added by low composition of dopant.

Based on the experiment result can be revealed that the optimum composition of all TiO_2-M was obtained at ratio 3:1. In addition, TiO_2-Cd was the best formulation compared to others TiO_2-M with degradation percentages of 92.83% followed by TiO_2-Co and TiO_2-Mn which they had degradation percentages of 91.64% and 89.79%, respectively as seen in Fig. 12.

The Cd, Co and Mn have different ionic radius inducing the resulted TiO_2-M. The ionic radiation of Cd^{2+} is larger than Co^{2+} and Mn^{2+}. The metals, which have large ionic radius, were doped into TiO_2 reducing the steric hydrant and make them easily to interact with oxygen thus a bonding with TiO_2 semiconductor was effortlessly achieved. The Mn, however, has small ionic radius causing the entrance to TiO_2 difficult to accomplish due to it has high steric hydrant.

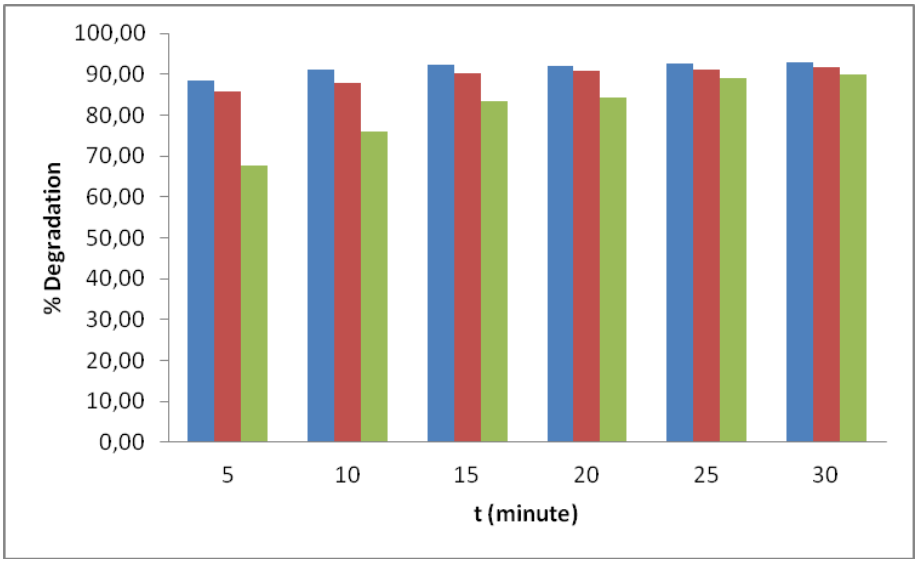

Figure 12. Methylene blue photocatalytic degradation percentages by TiO_2-Cd (3:1, blue), TiO_2-Co (3:1, red), TiO_2-Mn (3:1, green)

The photocatalytic activity was also influenced by oxidation number where the oxidation number of Cd < Co < Mn. The more of oxidation number of metals affected the number of species also more diverse thus the formed catalyst became irregular. This generated that TiO_2-Mn has low degradation percentages than others. Moreover, the band gap energy of TiO_2-Cd > TiO_2-Co > TiO_2-Mn also influenced in the photocatalytic activity because of the broad band gab will slow down electron-hole recombination process. All of that metals have reduction potential, where Cd < Co < Mn. The lower of their reduction potential, the more easily they oxidized and more stable in excitation state thus the number of empty orbital as an electron trap increased and recombination process became longer.

Photocatalyst degradation process was determined by reaction rate constant values (k) to identify the reaction kinetic on methylene blue degradation following first, second and third order reaction using Eqs. (1-3), respectively. From the first, second and third order reaction graphs was pointed the linearity value (R^2). The R^2 value closing to 1 showed the occurring order reaction and degradation of methylene blue. The k and R value of TiO_2-M was presented in Table 4.

$$\ln C = -k.t + \ln Co \quad (1)$$

$$\frac{1}{C} = k.t + \frac{1}{Co} \quad (2)$$

$$\frac{1}{C^2} - \frac{1}{Co^2} = 2k.t \quad (3)$$

Table 4. The reaction rate constant (*k*) and R values of methylene blue photocatalyst degradation by TiO_2-M 3:1

	Kinetic model	k (ppm.menit-1)	R2
TiO_2-Cd (3:1)	First order	0,0162	0,734
	Second order	0,0354	0,771
	Third order	0,0786	0,805
TiO_2-Mn (3:1)	First order	0,0469	0,963
	Second order	0,0542	0,967
	Third order	0,0682	0,930
TiO_2-Co (3:1)	First order	0,0089	0,972
	Second order	0,0152	0,975
	Third order	0,0261	0,975

Conclusion

Synthesis of TiO_2 and TiO_2-M (M = Cd, Co and Mn) have been successfully conducted through sol-gel method. The addition of metals influenced on not only

the TiO_2 crystal growth but also the material electronic properties (Eg TiO_2 = 3,35 eV; TiO_2-Cd = 3,15 eV; TiO_2-Co = 3 eV dan TiO_2-Mn = 2,5 eV). The more metals ion doped into TiO_2 semiconductor affected on decreasing of photocatalytic activity. It was revealed that the optimum composition of TiO_2-M was obtained at TiO_2:M ratio by 3:1. The TiO_2-Cd optimum photocatalytic degradation value was 92.56% followed by TiO_2-Co (90.44%) and TiO_2-Mn (89.42%) making it to be the best TiO_2-M composition compared to others.

REFERENCES

Alzaydien, A.S. (2009). Adsorption of methylene blue from aqueous solution onto a low- cost natural Jordanian Tripoli. *Amer. J. Environ. Sci.*, *5*, 197 – 208.

Binas, V.D., Sambani, K., Maggos, T., Katsanaki, A. & Kiriakidis, G. (2012). Synthesis and photocatalytic activity of Mn-doped TiO_2 nanostructured powders under UV and visible light. *Appl. Catalysis B: Environmental*, *113 – 114*, 79 – 86.

Chen, X., Lou, Y., Dayal, S., Qiu, X., Krolicki, R., Burda, C. & Becker, J. (2005). Doped semiconductor nanomaterials. *J. Nanosci. & Nanotech.*, *5*, 1408 – 1420.

Deng, Q.R., Xia, X.H., Guo, M.L., Gao, Y. & Shao, G. (2011). Mn-doped TiO_2 nanopowders with remarkable visible light photocatalytic activity. *Materials Lett. 65*, 2051 – 2054.

El-Bahy, Z.M., Ismail, A.A. & Mohamed, R.M. (2009). Enhancement of titania by doping rare earth for photodegradation of organic dye (Direct Blue). *J. Hazardous Materials*, *166*, 138 – 143.

Ganesh, I., Gupta, A.K., Kumar, P.P., Chandra Sekhar, P.S., Radha, K., Padmanabham, G. & Sundararajan, G. (2012). Preparation and characterization of Co-doped TiO_2 materials for solar light induced current and photocatalytic applications. *Materials Chem. & Phys., 135*, 220 – 234.

Ge, L., Zuo, F., Liu, J., Ma, Q., Wang, C., Sun, D., Bartels, L. & Feng, P. (2012). Synthesis and efficient visible light photocatalytic hydrogen evolution of polymeric g-C_3N_4 coupled with CdS quantum dots. *J. Phys. Chem. C*, *116*, 13708 – 13714.

Hamadanian, M., Reisi-Vanani, A. & Majedi, A. (2010). Sol-gel peparation and characterization of Co / TiO_2 nanoparticles: application to the degradation of methyl orange. *J. Iranian Chem. Soc., 7*, S52 – S58.

Hamdaoui, O. & Chiha, M. (2007). Removal of methylene blue from aqueous solutions by wheat bran. *Acta Chim. Slov*, *54*, 407 – 418.

Kernazhitsky, L., Shymanovska, V., Gavrilko, T., Puchkovska, G., Naumov, V., Khalyavka, T., Kshnyakin, V., Chemyak, V. & Baran, J. (2010).

Optical and photocatalytic properties of titanium-manganese mixed oxides. *Materials Sci. & Eng. B, 175*, 48 – 55.

Kuvarega, A.T., Krause, R.W.M. & Mamba, B.B. (2011). Nitrogen/palladium-codoped TiO_2 for efficient visible light photocatalytic dye degradation. *J. Phys. Chem. C*, *115*, 22110 – 22120.

Li, H., Lei, Y., Huang, Y., Fang, Y., Xu, Y., Zhu, L. & Li, X. (2011). Photocatalytic reduction of carbon dioxide to methanol by Cu_2O/SiC nanocrystallite under visible light irradiation. *J. Natural Gas Chem.*, *20*, 145 – 150.

Li, X., Xia, T., Xu, C., Murowchick, J. & Chen, X. (2014). Synthesis and photoactivity of nanostructured CdS-TiO2 composite catalysts. *Catalysis Today*, *225*, 64 – 73.

Miao, Y., Zhai, Z., Jiang, L., Shi, Y., Yan, Z., Duan, D., Zhen, K. & Wang, J. (2014). Facile and new synthesis of cobalt doped mesoporous TiO_2 with high visible-light performance. *Powder Technology*, *266*, 365 – 371.

Ni, M., Leung, M.K.H., Leung, D.Y.C. & Sumathy, K.. (2007). A review and recent developments in photocatalytic water-splitting using TiO_2 for hydrogen production. *Renewable &Sustainable Energy Rev., 11*, 401 – 425.

Othman, I., Mohamed, R.M. & Ibrahem, F.M. (2007). Study of photocatalytic oxidation of indigo carmine dye on Mn-supported TiO_2. *J. Photochem. & Photobiology A: Chemistry*, *189*, 80 – 85.

Papadimitriou, V.C., Stefanopoulos, V.G., Romanias, M.N., Papagiannakopoulos, P., Sambani, K., Tudose, V. & Kiriakidis, G. (2011). Determination of photo-catalytic activity of un-doped and Mn-doped TiO_2 anatase powders on acetaldehyde under UV and visible light. *Thin Solid Films*, *520*, 1195 – 1201.

Purnawan, C., Wahyuningsih, S. & Kusuma, P.P. (2016). Photocatalytic and photoelectrocatalytic degradation of methyl orange using graphite / $PbTiO_3$ composite, *Indones. J. Chem. 16*, 347 – 352.

Shi, J.W., Yan, X., Cui, H. J., Zong, X., Fu, M. L., Chen, S. & Wang, L. (2012). Low-temperature synthesis of CdS/TiO_2 composite photocatalysts: influence of synthetic procedure on photocatalytic activity under visible light. *J. Mol. Catalysis A: Chemical*, *356*, 53 – 60.

Šurca Vuk, A., Ješe, R., Gaberščček, M., Orel, B. & Dražič, G. (2006). Structural and spectroelectrochemical (UV-vis and IR) studies of nanocrystalline sol-gel derived TiO_2 films. *Solar Energy Materials & Solar Cells*, *90*, 452 – 468.

Tian, J., Deng, H., Sun, L., Kong, H., Yang, P. & Chu, J. (2012). Effects of Co doping on structure and optical properties of TiO_2 thin films prepared by sol–gel method. *Thin Solid Films*, *520*, 5179 – 5183.

Wahyuningsih, S., Purnawan, C., Kartikasari, P.A. & Praistia, N. (2013). Visible light photoelectrocatalytic degradation of rhodamine B using a dye-sensitised TiO_2 electrode. *Chem. Papers*, *68*, 1248 – 1256.

Wang, L., Zhang, X., Zhang, P., Cao, Z. & Hu, J. (2015). Photoelectric conversion performances of Mn doped TiO_2 under >420nm visible light irradiation. *J. Saudi Chem. Soc.*, *19*, 595 – 601.

Wu, J.C.-S. & Chen, C.-H. (2004). A visible-light response vanadium-doped titania nanocatalyst by sol-gel method. *J. Photochem. & Photobiology A: Chemistry, 163*, 509 – 515.

Yang, X., Cao, C., Hohn, K., Erickson, L., Maghirang, R., Hamal, D. & Klabunde, K. (2007). Highly visible-light active C- and V-doped TiO_2 for degradation of acetaldehyde. *J. Catalysis*, *252*, 296 – 302.

Zaleska, A. (2008). Doped-TiO_2: a review. *Recent Patents on Engineering, 2,* 157 – 164.

✉ **Candra Purnawan (corresponding author)**
Analytical and Environmental Chemistry Research Group
Chemistry Department
Sebelas Maret University
Surakarta, Central Java
57126 Indonesia
E-mail: candra_pr@staff.uns.ac.id